

Accepted Manuscript

New imidazoquinoxaline derivatives: Synthesis, biological evaluation on melanoma, effect on tubulin polymerization and structure-activity relationships

Zahraa Zghaib, Jean-François Guichou, Johanna Vappiani, Nicole Bec, Kamel Hadj-Kaddour, Laure-Anaïs Vincent, Stéphanie Paniagua-Gayraud, Christian Larroque, Georges Moarbess, Pierre Cuq, Issam Kassab, Carine Deleuze-Masquéfa, Mona Diab-Assaf, Pierre-Antoine Bonnet

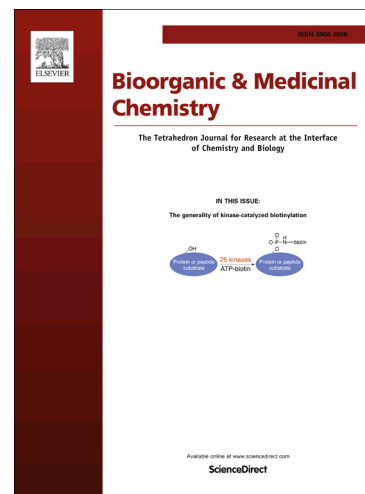
PII: S0968-0896(16)30226-7
DOI: <http://dx.doi.org/10.1016/j.bmc.2016.04.004>
Reference: BMC 12918

To appear in: *Bioorganic & Medicinal Chemistry*

Received Date: 11 December 2015
Revised Date: 25 March 2016
Accepted Date: 1 April 2016

Please cite this article as: Zghaib, Z., Guichou, J-F., Vappiani, J., Bec, N., Hadj-Kaddour, K., Vincent, L-A., Paniagua-Gayraud, S., Larroque, C., Moarbess, G., Cuq, P., Kassab, I., Deleuze-Masquéfa, C., Diab-Assaf, M., Bonnet, P-A., New imidazoquinoxaline derivatives: Synthesis, biological evaluation on melanoma, effect on tubulin polymerization and structure-activity relationships, *Bioorganic & Medicinal Chemistry* (2016), doi: <http://dx.doi.org/10.1016/j.bmc.2016.04.004>

This is a PDF file of an unedited manuscript that has been accepted for publication. As a service to our customers we are providing this early version of the manuscript. The manuscript will undergo copyediting, typesetting, and review of the resulting proof before it is published in its final form. Please note that during the production process errors may be discovered which could affect the content, and all legal disclaimers that apply to the journal pertain.



New imidazoquinoxaline derivatives: Synthesis, biological evaluation on melanoma, effect on tubulin polymerization and structure-activity relationships

Zahraa Zghaib^{1,2}, Jean-François Guichou^{3,4}, Johanna Vappiani¹, Nicole Bec⁵, Kamel Hadj-Kaddour¹, Laure-Anaïs Vincent¹, Stéphanie Paniagua-Gayraud¹, Christian Larroque⁵, Georges Moarbess², Pierre Cuq¹, Issam Kassab², Carine Deleuze-Masquéfa^{1*}, Mona Diab-Assaf², Pierre-Antoine Bonnet¹

¹ Institut des Biomolécules Max Mousseron (IBMM), UMR 5247, CNRS, Université de Montpellier, ENSCM, Faculté de Pharmacie, 15, avenue Charles Flahault, BP14491, 34093 Montpellier cedex 5, France

² Tumorigenèse et Pharmacologie Antitumorale, Lebanese University, BP 90656, Fanar Jdeideh, Lebanon.

³ CNRS, UMR5048 – Université de Montpellier, Centre de Biochimie Structurale, F-34090 Montpellier, France

⁴ INSERM, U1054, F-34090 Montpellier, France

⁵ IRCM, Institut de Recherche en Cancérologie de Montpellier, INSERM U896, 34298 Montpellier, France.

* Corresponding author. Tel.: +33 4 11 75 95 36; fax +33 11 75 95 53
E-mail adress: carine.masquefa@umontpellier.fr

Abstract

Microtubules are considered as important targets of anticancer therapy. **EAPB0503** and its structural imidazo[1,2-*a*]quinoxaline derivatives are major microtubule-interfering agents with potent anticancer activity. In this study, the synthesis of several new derivatives of **EAPB0503** is described, and the anticancer efficacy of 13 novel derivatives on A375 human melanoma cell line is reported. All new compounds show significant antiproliferative activity with IC_{50} in the range of 0.077-122 μ M against human melanoma cell line (A375). Direct inhibition of tubulin polymerization assay *in vitro* is also assessed. Results show that compounds **6b**, **6e**, **6g**, and **EAPB0503** highly inhibit tubulin polymerization with percentages of inhibition of 99%, 98%, 90%, and 84% respectively. Structure-activity relationship studies within the series are also discussed in line with molecular docking studies into the colchicine-binding site of tubulin.

Keywords: antiproliferative activity; tubulin depolymerization; human melanoma cancer cell line (A375); structure-activity relationship; molecular docking; imidazo[1,2-*a*]quinoxaline

1. Introduction

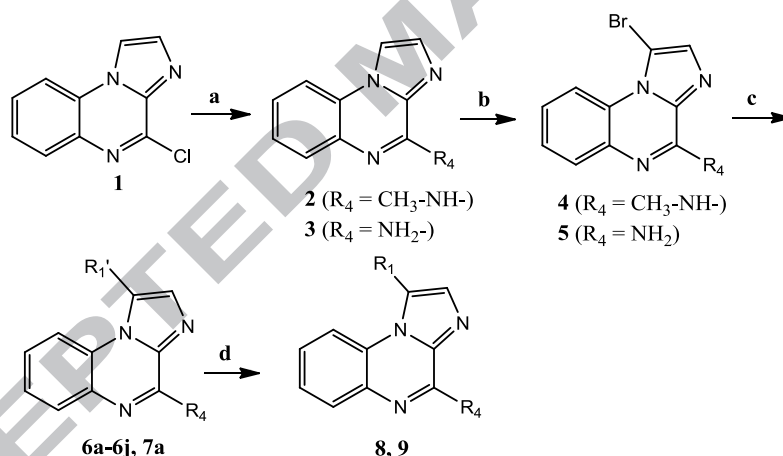
Microtubules are the key components of the cytoskeleton of eukaryotic cells and have an important role in various cellular functions such as mitosis, exocytosis, and maintenance of cellular morphology, active transport, cell shape and polarization.^{1,2} They play a critical role in cell division by their involvement in the movement and attachment of the chromosomes during various stages of mitosis. Therefore microtubule dynamics is an important target for the development of anti-cancer agents.³⁻⁵ Microtubules are composed of α/β tubulin heterodimers, always in a state of equilibrium.^{3,4} Microtubule targeting agents (MTA), drugs that interfere with microtubule dynamic stability, are widely employed in the clinic to treat a variety of cancers or are exploited as probes to gain insights into microtubule structure and function.⁴⁻¹⁰ MTAs are antimetabolic agents which perturb not only mitosis but also arrest cells during interphase. MTAs are known to interact with tubulin through at least four binding sites: the laulimalide, taxane/epothilone, vinca alkaloid, and colchicine sites.^{1,11} Colchicine binds to the intradimeric α - β interface of tubulin heterodimers contiguous to the GTP-binding domain of the α -tubulin subunit¹²⁻¹⁵ and the tubulin-colchicine complex prevents further polymerization of the microtubule. Such complex brings about a conformational change which blocks the tubulin dimers from further addition and prevents the growth of the microtubule by producing potent destabilization effects of microtubules, resulting in the subsequent shutdown of existing tumor vasculature.^{1,16}

Efforts have been increasing for new compounds exhibiting inhibition of tubulin assembly and disassembly in order to induce anti-proliferative activities and treat a wide variety of malignancies.¹⁷⁻²² The alteration of microtubule dynamics prevents cells division and apoptosis of different human cancer lines including Multi Drug Resistant (MDR) cancer cell lines.²³⁻²⁵

Imidazoquinoxalines derivatives have been designed by our laboratory since 2004 using different strategies of synthesis. Among these derivatives, **EAPB0203** and **EAPB0503** (Figure 1) have shown potent antitumor properties *in vitro* and *in vivo* against melanoma and T-cell lymphomas.²⁶⁻²⁹ Preliminary studies have shown antitubuline activity for those two derivatives.³⁰

optimize the time of reactions, purity of the intermediates, and global yields. It is also to be noted that the synthesis of the parent compound **1** can also be optimized using microwave assistance by treating the 4,5-lactame derivative precursor with phosphorus oxychloride and *N,N*-diethylaniline in a sealed vial using a Biotage® initiator microwave synthesizer. Nevertheless, the crude compound obtained still requires further purification on silica gel column chromatography for the next steps of the synthetic scheme.

First diversity on position 4 is obtained by substitution of the chlorine on compound **1** by the appropriate amine under microwave heating to give compounds **2** and **3**. The bromination on position 1 of compounds **2** and **3** by *N*-bromosuccinimide under microwave conditions leads to compound **4** and **5**, respectively. In comparison to the initial synthetic procedure,²⁶⁻²⁸ steps *a* and *b* (Scheme 1) as well as the step leading to the parent compound **1**, have been optimized using microwave irradiation instead of conventional heating.



Scheme 1: Synthesis of EAPB0503 derivatives. a) EtOH, NH_2CH_3 in ethanol or NH_4OH in water, MW (180°C , 20 min); b) NBS, CHCl_3 , reflux 1h30; c) Suzuki-cross coupling ($\text{R}_1'\text{-B(OH)}_2$), $\text{Pd(PPh}_3)_4$, Na_2CO_3 , DME, MW (140°C , 20 min); d) Iodocyclohexane, DMF, reflux 16h.

A second step for diversity is obtained using different arylboronic acids in Suzuki-cross coupling reactions. As expected, the palladium catalyzed substitution selectively occurs on the bromo position to obtain compounds **6a** to **6j**, and **7a** under microwave assistance (140°C , 20 min) with good to acceptable yields. The phenol derivatives **8** and **9** can be obtained by a treatment of the methoxy compounds **EAPB0503** and **7a** with iodocyclohexane under conventional heating. Compounds **2** to **4**, **EAPB0503**, **6a** and **6b** were described with their analytical data in previous studies.²⁶⁻²⁸

2.2. Biological evaluation

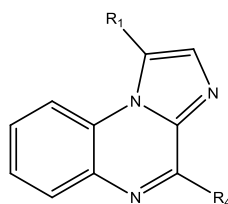
2.2.1. *In vitro* cell growth inhibition

All compounds were tested for their cytotoxic effect on human melanoma cell line (A375), our *in vitro* model used previously for screening,²⁶⁻²⁸ using **EAPB0503** as reference, which showed previously an important cytotoxic activity comparing to fotemustine, clinically used for human melanoma treatment.²⁶⁻²⁸ The screening results reported in Table 1 demonstrate that all our new compounds showed significant antiproliferative activity with IC₅₀ in the range of 0.077-122 μ M against human melanoma cell line used. Compounds **6b**, **6d**, **6e**, **6g**, **7a** and **8** were distinctly more potent from the other compounds. However, **6g** was the only compound presenting the highest significant antiproliferative activity in comparison to **EAPB0503** ($P=0.002<0.05$). It displayed an IC₅₀ values about 0.077 μ M, 3 time-folds more potent than **EAPB0203** (0.2 μ M). Compound **6a** showed the lowest cytotoxic activity ($P<0.05$). Based on the cytotoxicity data, the structure-activity relationship (SAR) for these new imidazoquinoxaline derivatives was examined. It is interesting to observe that the compounds with a methoxy or hydroxy substitution at *meta*-position (**7a**, **8** and **9**), and the dimethoxy substitutions at 3,4 or 3,5 and 3,6 positions (**6d**, **6e**, and **6f**) on the phenyl ring (R1) showed similar or slightly reduced activity on A375 cancer cell in comparison to **EAPB0503**. Moderate decrease in activity than **EAPB0503** was observed for the trimethoxy substituted compounds (**6h**, **6i** and **6j**). The *ortho*-methoxy substitution (**6a**) showed an important decrease in the cytotoxic activity. It is important to note that the 2-hydroxy-3-methoxy compound (**6g**) presented the most important antiproliferative activity. These findings conducted us to highlight that at least one methoxy or hydroxy substitution at *meta*-position on the phenyl ring is recommended to maintain the cytotoxic activity of these derivatives.

2.2.2. *In vitro* effect on tubulin polymerization

To investigate whether the antiproliferative activities of these compounds were related or not to the interaction with tubulin and in order to more investigate the mechanism of action of our derivatives, we evaluated their capacity for binding and inhibiting tubulin polymerization. For this issue, tubulin was purified from pig brain tissue according the protocol described in the experimental part. Colchicine, a known natural antitubuline inhibitor, was used as reference. The results on tubulin polymerization are illustrated in Table 1.

Table 1: Imidazoquinoxaline derivatives: general formula, IC₅₀ values against A375 cells and effect on tubulin polymerization inhibition.



Compounds	R1	R4	IC ₅₀ ^a (μM) on A375 ^b	% of tubulin polymerization inhibition /DMSO 5 μM ^c
EAPB0503	3-OCH ₃ -C ₆ H ₄ -	CH ₃ -NH-	0.2 ± 0.02	84.0 ± 3.2
6a	2-OCH ₃ -C ₆ H ₄ -	CH ₃ -NH-	122 ± 25	0
6b	4-OCH ₃ -C ₆ H ₄ -	CH ₃ -NH-	0.37 ± 0.4	99.0 ± 3.4
8	3-OH-C ₆ H ₄ -	CH ₃ -NH-	1.25 ± 0.18	0
7a	3-OCH ₃ -C ₆ H ₄ -	H ₂ N-	0.20 ± 0.0014	41.0 ± 7.8
9	3-OH-C ₆ H ₄ -	H ₂ N-	2.4 ± 0.6	11.33 ± 6.3
6c	2,3-di-OCH ₃ -C ₆ H ₃ -	CH ₃ -NH-	5.9 ± 0.3	0
6d	3,4-di-OCH ₃ -C ₆ H ₃ -	CH ₃ -NH-	0.3 ± 0.003	63.0 ± 8.0
6e	3,5-di-OCH ₃ -C ₆ H ₃ -	CH ₃ -NH-	0.22 ± 0.005	98.5 ± 4.0
6f	2,5-di-OCH ₃ -C ₆ H ₃ -	CH ₃ -NH-	1.20 ± 0.044	3.0 ± 2.4
6g	2-OH-3-OCH ₃ -C ₆ H ₃ -	CH ₃ -NH-	0.077 ± 0.005	90.0 ± 7.7
6h	2,3,4-tri-OCH ₃ -C ₆ H ₃ -	CH ₃ -NH-	1.50 ± 0.30	0
6i	3,4,5-tri-OCH ₃ -C ₆ H ₂ -	CH ₃ -NH-	1.80 ± 0.38	0
6j	2,4,6-tri-OCH ₃ -C ₆ H ₂ -	CH ₃ -NH-	2.30 ± 0.09	0
Colchicine			0.010 ± 0.002	52 ± 5

IC₅₀: compound concentration required for A375 growth inhibition by 50%; ^a Values are derived from three independent experiments, the standard deviation are also noted; ^bA375 human melanoma cells. ^c Values are expressed in percentages, derived from three independent experiments and the SD are also calculated.

Compounds **6b**, **6e**, **6g**, and **EAPB0503** (at 5 μM) were highly effective in their ability to inhibit tubulin assembly with percentages of inhibition values of 99%, 98%, 90% and 84%, respectively. These compounds exhibited significant high potency on tubulin inhibition in comparison with colchicine which demonstrated a percentage up to 52% of inhibition ($P = 0.01, 0.01, 0.04, \text{ and } 0.02$ respectively < 0.05). The high effect on tubulin inhibition is correlated with their potent antiproliferative effect on human melanoma cell line. This reported data showed an important role of these derivatives as antiproliferative and antimetabolic agents. Based on the structural analogy with colchicine, we decided to introduce methoxy groups, presents on colchicine, on our compounds to improve their antitubulin inhibition. Surprisingly, compounds (**6a**, **6h**, **6i**, and **6j**) bearing three methoxy substitutions did not show any inhibition of tubulin assembly.

2.2.3. EAPB0503, 6b and 6e causes G2/M cell-cycle arrest

Cellular DNA contents were determined by Flow cytometer analysis on cell treatment. **EABP0503**, **6b** and **6e** induced significant dose-dependent changes in the cell-cycle distribution (Figure 2). Indeed, all 3 compounds induce a dramatic blockage in G2/M phase. Those results were agreed to those of antitubulinic agents that usually caused a block of cells in the G2/M phase of the cell cycle. In fact, their ability to inhibit tubulin assembly will avoid the mitotic spindle formation and so the mitosis.

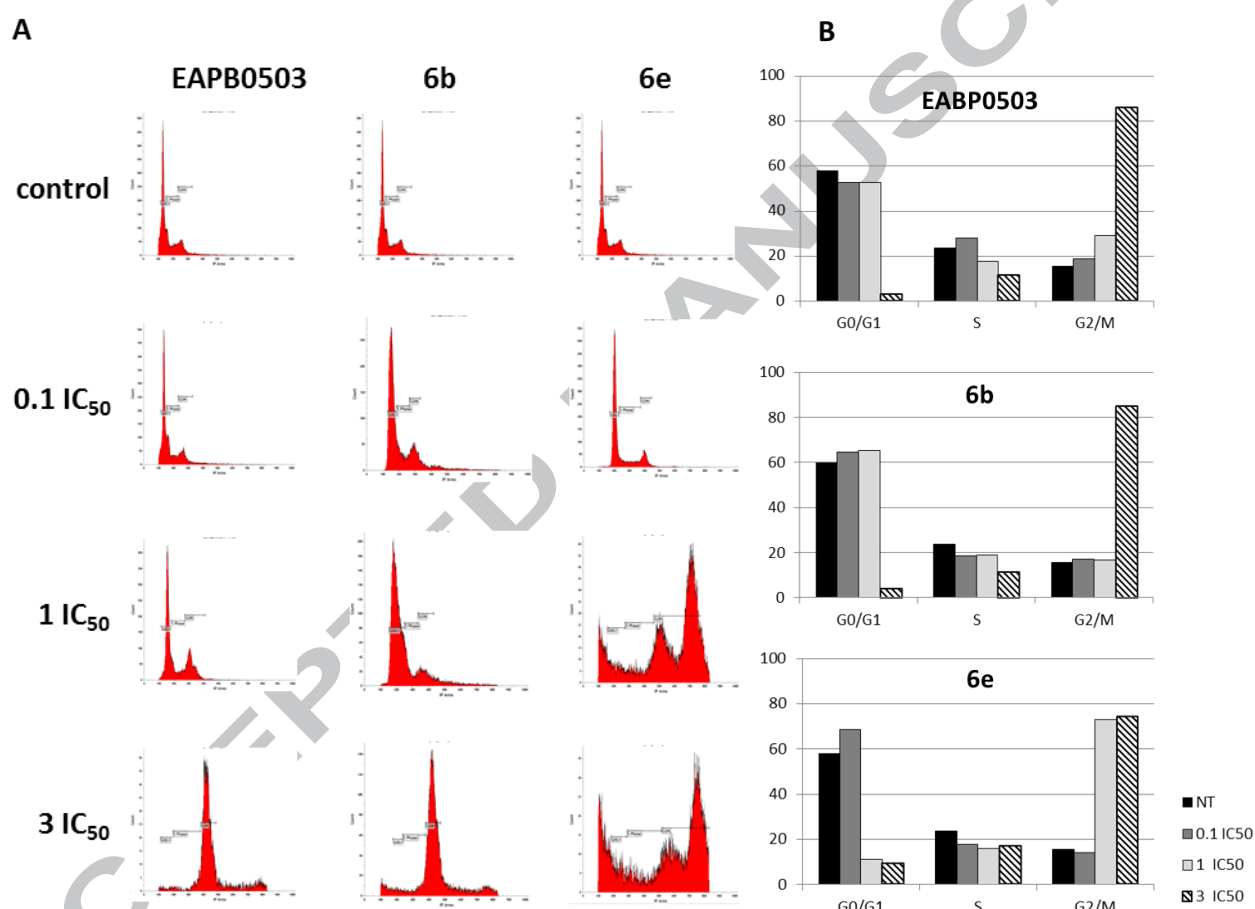


Figure 2: EABP0503, 6b and 6e induce G2/M cell arrest on A375 cell line. (A) Effects of **EABP0503**, **6b** and **6e** on the cell-cycle distribution on A375 cell line. Treated cells were stained with PI (25 $\mu\text{g/ml}$), and the cell-analysis was performed by a Gallios flow cytometer. (B) The G0/G1, S and G2/M percentage measured in treated cells.

2.3. Molecular Modeling

In order to better precise and in line with SAR the tubulin affinity and selectivity of our compounds, molecular docking simulations were determined with this series of compounds. The 3D structures of all chemical compounds were generated using PRODRG interface.³¹ Molecular docking studies were performed using the GOLD software³² to examine a possible

binding mode of all compounds in the colchicine binding domains of tubulin. Colchicine binds between the two chains (α and β) of tubulin making a hydrogen bond with Val181 of chain β ³³ and a hydrogen bond with Thr353 of chain α connected with a water molecule (Figure 3a). The tri-methoxyphenyl ring of colchicine is buried in a hydrophobic pocket of chain α form by the side chain of residues Cys241, Leu242, Leu248, Ala250, Leu255, Ile318, Ala354 and Ile378 (Figure 3a). The tropolone ring of colchicine is at the entrance of this pocket and made Van der Waals interactions with the side chain of residues Leu255, Met259, Ala316 and Lys352. Docking studies of all compounds into the colchicine site of tubulin showed a good correlation with the inhibition of tubulin polymerization. As an example, compounds **6a**, **6c**, **6h**, **6i** and **6j** could not be docked in this colchicine site and demonstrated absence of tubulin polymerization inhibition. On the contrary, compounds **EAPB0503**, **6b**, **6e**, **6g** and **7a** could be docked in the colchicine site. Compound **6g** with the highest activity on A375 cells showed a good superimposition of the tropolone ring with the phenyl substituted (Figure 3b-d) by making a hydrogen bond with Val181 of chain β as the colchicine. Imidazoquinoxaline ring made a hydrogen bond with residue Asn101 from chain β and Van der Waals interaction with Leu255, Met259, Ala316 and Lys352 from chain α . These findings suggested that compound **6g** does not mimic the tri-methoxyphenyl ring of the colchicine fitting into the hydrophobic pocket of chain α . This result can explain the inactivity of compounds **6h**, **6i** and **6j** bearing three methoxy groups on the phenyl ring due to clash with Met259.

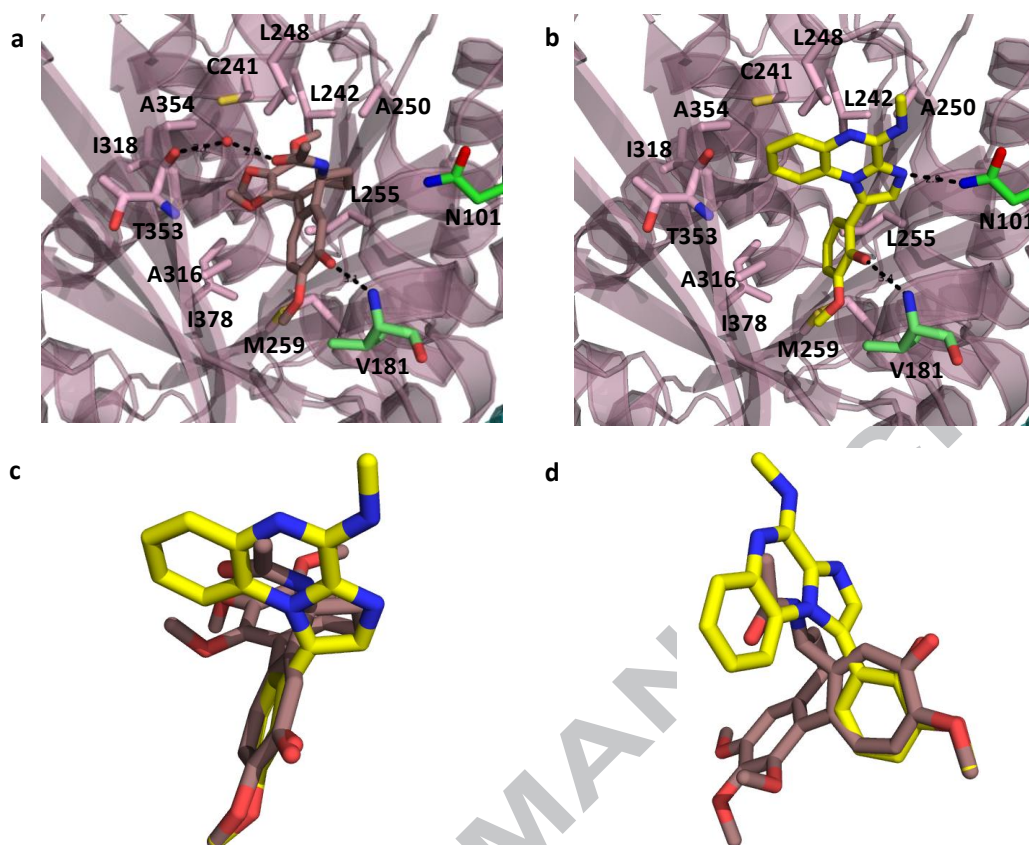


Figure 3: Compound **6g** in the colchicine binding pocket of tubulin chains α and β . **a.** Structure of tubulin with colchicine bound PDB 4O2B; **b.** Hydrogen bonds interaction between compound **6g** and tubulin (view from the top of the ligand); **c.** Superposition of compound **6g** and colchicine (view from the top). **d.** Superposition of compound **6g** and colchicine (view from the side); Color coding: nitrogen atoms blue, oxygen atoms red, carbon atoms pale pink for tubulin chain α , carbon atoms green for tubulin chain β , carbon atoms yellow for compound **6g** and brown for colchicine; Hydrogen bonds were showed by black dash-line, the distance was denoted by Å; water molecule is shown as non-bond sphere.

The results obtained from the docking simulations provided us a general binding mode that was able to justify the biological activity of the compounds and gave some indication for further rational improvement of imidazoquinoxaline derivatives.

3. Conclusion

A library of new heterocyclic compounds, imidazo[1,2-*a*]quinoxaline derivatives were synthesized under microwave assistance. The total reaction time and the yield of the products have been optimized comparing to the conventional heating. These new derivatives exhibited remarkable antiproliferative effects on human melanoma cell lines (A375). Compound **6g** presented the most important antiproliferative activity. SAR studies showed that at least one methoxy or hydroxy substitution at *meta*-position on the phenyl ring is mandatory to maintain

the cytotoxic activity of these derivatives. Compounds **6b**, **6e**, **6g**, and **EAPB0503**, showed potent inhibitions of the tubulin polymerization which are correlated to the antiproliferative activities. Compound **6g** is able to make a hydrogen bond with Val181 of chain β as colchicine and another hydrogen bond with residue Asn101 from chain β and Van der Waals interaction with Leu255, Met259, Ala316 and Lys352 from chain α . On the basis of these important properties, these derivatives can be promising leads in the development of anticancer agents.

4. Experimental

4.1. Chemistry

All solvents and reagents were obtained from commercial sources and used without further purification unless indicated otherwise. ^1H and ^{13}C NMR spectra were recorded using a Bruker AC 400 or 300 spectrometer. Chemical shifts are reported in parts per million (ppm) from the tetramethylsilane resonance in the indicated solvent. Coupling constants are reported in Hertz (Hz), spectral splitting partners are designed as follow: (s) singlet, (br s) broad singlet, (d) doublet, (dd) doublet of doublets (t) triplet, (td) triplet of doublets, (m) multiplet. High Resolution Mass Spectra (HRMS) (ElectroSpray Ionization method (ESI) and Q-ToF high resolution) were recorded on Synapt G2-S (Waters) by the physical measure department (IBMM, Montpellier, France). Column chromatography was performed on Aldrich silica gel 60 (230–400 mesh). The microwave organic synthesis was assisted by the Biotage® initiator (Temperature range: 40 - 300°C; Pressure range: 0 – 30 bar; Power range: 0 - 400 W from magnetron at 2.45 GHz).

4.1.1. Imidazo[1,2-a]quinoxalin-4-amine (**3**)

NH_4OH of a 33% (w/v) aqueous solution (2.7 mL, 19.7 mmol) was added to a solution of **1** (0.500 g, 2.5 mmol) in acetonitrile (5 mL). The mixture was placed under microwave heating at 180°C during 20 min. The solvent was removed under reduced pressure, and the residue was dissolved in CH_2Cl_2 (20 mL). The organic fraction was successively washed with saturated NaCl solution (15 mL) and water (15 mL), dried (Na_2SO_4), and concentrated under reduced pressure. The product was obtained (yield, 94 %) and used without purification. ^1H NMR (300 MHz, DMSO-d_6) δ : 7.92 (d, 1H), 7.79 (d, 1H), 7.72 (m, 2H), 7.65 (m, 2H), 6.66

(br s, 2H); ^{13}C NMR (300 MHz, DMSO- d_6) δ : 142.49, 131.92, 129.26, 128.88, 127.58, 125.81, 125.26, 124.72, 114.26, 111.75.

4.1.2. 1-bromoimidazo[1,2-a]quinoxalin-4-amine (**5**)

A solution of **3** (1.25 g, 6.8 mmol) and *N*-bromosuccinimide (1.3 g, 7.5 mmol) in CHCl_3 (200 mL) was heated under reflux for 1h30. The resulting solution was cooled, washed with 5% sodium hydrogen carbonate (50 mL), dried with Na_2SO_4 and concentrated under reduced pressure. Yield 80%. ^1H NMR (300 MHz, DMSO- d_6) δ : 7.95 (d, 1H), 7.75 (m, 2H), 7.71 (m, 1H), 7.68 (m, 1H), 6.65 (br s, 2H); ^{13}C NMR (300 MHz, DMSO- d_6) δ : 142.20, 138.78, 129.66, 128.16, 127.17, 126.95, 126.18, 125.51, 113.98, 99.27. HRMS: m/z calcd for $\text{C}_{11}\text{H}_{10}\text{N}_4\text{Br}$ [M] $^+$ 277.0089; Found 277.0088.

General procedure for the Suzuki cross-coupling reaction²¹⁻²³

The Suzuki coupling of **4** (300 mg, 1.09 mmol) or **5** with the corresponding aryl boronic acid in the presence of palladium catalyst $\text{Pd}(\text{PPh}_3)_4$ (60 mg), basic conditions Na_2CO_3 (250 mg), DME (10 mL), H_2O (5 mL) and under microwave assistance (140°C, 20 min) led to **6c-6j** and **7a**. These compounds were purified by column chromatography on silica gel, leading to the pure desired products.

4.1.3. 1-(2,3-dimethoxyphenyl)-*N*-methylimidazo[1,2-a]quinoxalin-4-amine (**6c**)

2,3-dimethoxyphenyl boronic acid (218 mg, 1.2 mmol). Yellow solid (66%). ^1H NMR (400 MHz, CDCl_3) δ : 7.80 (d, $J = 8$ Hz, 1H), 7.43 (s, 1H), 7.32-7.10 (m, 4H), 7.02-6.90 (m, 2H), 6.28 (br s, 1H), 3.95 (s, 3H), 3.55 (s, 3H), 3.28 (d, 3H). ^{13}C NMR (400 MHz, CDCl_3) δ : 153.07, 148.16, 137.72, 133.95, 132.28, 126.91, 126.68, 126.17, 125.23, 124.32, 123.68, 122.68, 115.58, 114.26, 60.72, 55.98, 27.87. HRMS: m/z calcd for $\text{C}_{19}\text{H}_{19}\text{N}_4\text{O}_2$ [M] $^+$ 335.1508; Found 335.1510.

4.1.4. 1-(3,4-dimethoxyphenyl)-*N*-methylimidazo[1,2-a]quinoxalin-4-amine (**6d**)

3,4-dimethoxyphenyl boronic acid (218 mg, 1.2 mmol). Off white solid (30%). ^1H NMR (400 MHz, CDCl_3) δ : 7.87 (d, $J = 8$ Hz, 1H), 7.44 (s, 1H), 7.38-7.35 (m, 2H), 7.13-6.97 (m, 4H), 6.50 (br s, 1H), 3.96 (s, 3H), 4.02 (s, 3H), 3.89 (s, 3H), 3.37 (br s, 3H). ^{13}C NMR (400 MHz, CDCl_3) δ : 149.99, 149.11, 148.28, 138.02, 133.66, 132.06, 130.73, 127.11, 125.82, 123.19,

122.81, 122.37, 115.98, 113.39, 111.28, 56.08, 56.03, 27.59. HRMS: m/z calcd for $C_{19}H_{19}N_4O_2$ [M]⁺ 335.1508; Found 335.1510.

4.1.5.1-(3,5-dimethoxyphenyl)-N-methylimidazo[1,2-a]quinoxalin-4-amine (6e)

3,5-dimethoxyphenyl boronic acid (218 mg, 1.2 mmol). Yellow solid (40%). ¹H NMR (400 MHz, CDCl₃) δ : 7.79 (d, J = 8 Hz, 1H), 7.37-7.26 (m, 3H), 6.94 (td, 1H), 6.59-6.56 (m, 3H), 6.43 (br s, 1H), 3.75 (s, 6H), 3.29 (br s, 3H). ¹³C NMR (400 MHz, CDCl₃) δ : 161.05, 132.24, 126.64, 123.02, 116.33, 108.29, 55.58, 28.11. HRMS: m/z calcd for $C_{19}H_{19}N_4O_2$ [M]⁺ 335.1508; Found 335.1505.

4.1.6. 1-(2,5-dimethoxyphenyl)-N-methylimidazo[1,2-a]quinoxalin-4-amine (6f)

2,5-dimethoxyphenyl boronic acid (218 mg, 1.2 mmol). White solid (83%). ¹H NMR (400 MHz, CDCl₃) δ : 7.86 (d, J = 4 Hz, 1H), 7.44 (s, 1H), 7.38-7.28 (m, 2H), 7.11-6.96 (m, 4H), 6.51 (br s, 1H), 3.85 (s, 3H), 3.58 (s, 3H), 3.37 (br s, 3H). ¹³C NMR (400 MHz, CDCl₃) δ : 153.55, 152.34, 147.89, 132.25, 126.36, 122.72, 120.15, 117.63, 116.07, 115.54, 112.00, 55.89, 55.84, 28.08. HRMS: m/z calcd for $C_{19}H_{19}N_4O_2$ [M]⁺ 335.1508; Found 335.1509.

4.1.7. 1-(2-hydroxy-3-methoxyphenyl)-N-methylimidazo[1,2-a]quinoxalin-4-amine (6g)

2-hydroxy-3-methoxyphenyl boronic acid (201 mg, 1.2 mmol). White solid (9%). ¹H NMR (300 MHz, CDCl₃) δ : 7.80 (br s, 1H), 7.41 (s, 1H), 7.36-7.26 (m, 2H), 7.06-6.93 (m, 4H), 6.35 (br s, 1H), 6.05 (br s, 1H), 3.96 (s, 3H), 3.27 (br s, 3H). ¹³C NMR (300 MHz, CDCl₃) δ : 146.32, 143.50, 142.84, 139.57, 131.13, 130.76, 129.38, 129.02, 125.91, 124.90, 124.47, 121.72, 121.48, 117.99, 114.94, 108.52, 55.93, 29.30. HRMS: m/z calcd for $C_{18}H_{17}N_4O_2$ [M]⁺ 321.1352; Found 321.1354.

4.1.8. 1-(3-methoxyphenyl)imidazo[1,2-a]quinoxalin-4-amine (7a)

5 (320 mg, 1.21 mmol), 3-methoxyphenyl boronic acid (370 mg, 2.4 mmol). Yield 79%. ¹H NMR (300 MHz, CDCl₃) δ : 7.98 (s, 1H), 7.65 (m, 2H), 7.55 (m, 2H), 7.3 (m, 2H), 6.97 (m, 2H), 6.2 (br s, 2H), 3.52 (s, 3H). ¹³C NMR (300 MHz, CDCl₃) δ : 160.89, 143.10, 131.06, 130.68, 129.88, 129.73, 128.27, 127.39, 126.20, 125.02, 124.86, 119.97, 118.73, 115.08, 111.87, 108.79, 55.30. HRMS: m/z calcd for $C_{17}H_{15}N_4O$ [M]⁺ 291.1246; Found 291.1251.

4.1.9. N-methyl-1-(2,3,4-trimethoxyphenyl)imidazo[1,2-a]quinoxalin-4-amine (6h)

2,3,4-trimethoxyphenyl boronic acid (365 mg, 2.17 mmol). Yellow solid (15%). ^1H NMR (400 MHz, CDCl_3) δ : 7.80 (br s, 1H), 7.35-7.19 (m, 3H), 7.05 (d, $J = 8$ Hz, 1H), 6.95-6.88 (m, 1H), 6.74 (d, $J = 8$ Hz, 1H), 3.91 (s, 3H), 3.85 (s, 3H), 3.53 (s, 3H), 3.30 (br s, 3H). ^{13}C NMR (400 MHz, CDCl_3) δ : 154.61, 151.73, 146.64, 141.37, 131.13, 131.03, 125.31, 121.88, 114.49, 106.14, 60.05, 59.86, 55.12, 28.67. HRMS: m/z calcd for $\text{C}_{20}\text{H}_{21}\text{N}_4\text{O}_3$ $[\text{M}]^+$ 365.1614; Found 365.1615.

4.1.10 *N*-methyl-1-(3,4,5-trimethoxyphenyl)imidazo[1,2-*a*]quinoxalin-4-amine (**6i**)

3,4,5-trimethoxyphenyl boronic acid (365 mg, 2.17 mmol). Yellow solid (28%). ^1H NMR (400 MHz, CDCl_3) δ : 7.76 (d, $J = 8$ Hz, 1H), 7.36 (s, 1H), 7.31-7.26 (m, 2H), 6.93 (td, 1H), 6.66 (s, 2H), 6.38 (br s, 1H), 3.90 (s, 3H), 3.78 (s, 6H), 3.26 (br s, 3H). ^{13}C NMR (400 MHz, CDCl_3) δ : 153.54, 147.92, 138.99, 132.10, 128.34, 125.47, 122.73, 119.10, 116.15, 107.56, 61.12, 56.32, 27.97. HRMS: m/z calcd for $\text{C}_{20}\text{H}_{21}\text{N}_4\text{O}_3$ $[\text{M}]^+$ 365.1614; Found 365.1616.

4.1.11. *N*-methyl-1-(2,4,6-trimethoxyphenyl)imidazo[1,2-*a*]quinoxalin-4-amine (**6j**)

2,4,6-trimethoxyphenyl boronic acid (365 mg, 2.17 mmol). Yellow solid (20%). ^1H NMR (400 MHz, CDCl_3) δ : 7.70 (d, $J = 8$ Hz, 1H), 7.30-7.21 (m, 3H), 6.88 (td, 1H), 6.41 (br s, 1H), 6.18 (s, 2H), 3.86 (s, 3H), 3.56 (s, 6H), 3.22 (br s, 3H). ^{13}C NMR (400 MHz, CDCl_3) δ : 163.06, 160.18, 148.20, 132.16, 132.06, 126.41, 125.90, 122.62, 115.04, 114.45, 100.45, 90.78, 55.79, 55.53, 27.77. HRMS: m/z calcd for $\text{C}_{20}\text{H}_{21}\text{N}_4\text{O}_3$ $[\text{M}]^+$ 365.1614; Found 365.1613.

General procedure for the demethylation reaction

To **EAPB0503** and **7a** under nitrogen atmosphere in anhydrous dimethylformamide, iodocyclohexane was added to the mixture and the reactions were heated to reflux for 16 h. Iced water (20 mL) was added to the residues and the products were extracted with CH_2Cl_2 (3 x 30 mL). The combined organic extracts were washed with water (40 mL), dried (Na_2SO_4) and concentrated to dryness under reduced pressure. The crude products were purified by column chromatography on silica gel using C_6H_{12} -EtOAc (50:50 v/v) as eluent, leading to products, which were then taken into chloroform at 0°C , filtrated and washed with iced chloroform, yielding to the pure compounds **8** and **9**.

4.1.12. 3-(4-methylamino)imidazo[1,2-*a*]quinoxalin-1-ylphenol (**8**)

EAPB0503 (200 mg, 0.64 mmol), dimethylformamide (2 mL), iodocyclohexane (3.3 mmol, 0.424 mL). Yield 22%. ^1H NMR (300 MHz, MeOD) δ : 9.84 (br s, 2H), 7.78 (dd, 1H), 7.62 (dd, 1H), 7.4 (m, 2H), 7.35 (m, 1H), 7.29 (m, 2H), 6.85 (m, 2H), 3.25 (s, 3H), ^{13}C NMR (300 MHz, CDCl_3) δ : 160.07, 142.83, 139.57, 131.46, 131.13, 130.35, 129.59, 129.02, 126.92, 124.90, 124.47, 122.10, 117.66, 114.96, 114.43, 112.32, 29.32. HRMS: m/z calcd for $\text{C}_{17}\text{H}_{15}\text{N}_4\text{O}$ $[\text{M}]^+$ 291.1246; Found 291.1245.

4.1.13. 3-(4-amino)imidazo[1,2-a]quinoxalin-1-yl)phenol (**9**)

7a (200 mg, 0.689 mmol), dimethylformamide (5 mL), iodocyclohexane (8.26 mmol, 1.00 mL). Yield 17%. ^1H NMR (300 MHz, MeOD) δ : 9.88 (br s, 3H), 7.55 (m, 2H), 7.45 (m, 2H), 7.32 (m, 2H), 7.20 (s, 1H), 6.98 (m, 2H). ^{13}C NMR (300 MHz, CDCl_3) δ : 160.07, 143.10, 131.58, 131.06, 130.35, 129.35, 129.97, 129.97, 129.73, 126.78, 126.20, 125.02, 124.85, 119.97, 118.37, 115.08, 114.43, 113.03. HRMS: m/z calcd for $\text{C}_{16}\text{H}_{13}\text{N}_4\text{O}$ $[\text{M}]^+$ 277.1089; Found 277.1093.

4.2. Biological evaluation

4.2.1. Materials and reagents.

Compounds and reactants used in this study were bought from Sigma-Aldrich (Saint-Quentin Fallavier, France). 3-(4,5-dimethylthiazol-2-yl)-2,5-diphenyltetrazolium bromide (MTT), isopropyl alcohol and chlorhydric acid were obtained from Merck (Darmstadt, Germany). All other reagents were of analytical grade and were obtained from commercial sources. Statistical analysis for the values was performed using t-test and P values are calculated. Probably values of less than 0.05 were considered statistically significant.

4.2.2. Cell lines and culture techniques.

Melanoma human cancer cell line (A375) was obtained from American Type Culture Collection (Rockville, Md., USA). Cells were cultured in RPMI medium containing RPMI-1640 (LONZA, Basel, Switzerland), supplemented with 10% heat-inactivated (56°C) foetal bovine serum (FBS) (Gibco, Waltham, MA, USA), 2 mM L-glutamine, 100 IU/ml penicillin G sodium, 100 $\mu\text{g}/\text{ml}$ streptomycin sulphate and 0.25 $\mu\text{g}/\text{ml}$ amphotericin B. Cells were maintained in a humidified atmosphere of 5% CO_2 in air at 37 °C.

4.2.3. Cytotoxicity Assay.

Previously to the experiments, the number of cells by well, the doubling time and the MTT concentration have been optimized. In all the experiments, A375 were seeded at a final concentration of 5000 cells/well in 96-well microtiter plates and allowed to attach overnight. After 20-24 hours incubation, the medium was aspirated carefully from the plates using a sterile Pasteur pipette, and cells were exposed i) to vehicle controls (1% DMSO/culture medium and culture medium alone), ii) to **EAPB0503**, of 10^{-4} to 10^{-10} μM , diluted in the culture medium, and iii) to the synthesized compounds (10^{-4} - 10^{-10} μM) dissolved in a mixture 1% DMSO/culture medium (v/v). After 96 h of incubation, 10 μl of MTT solution in PBS (5 mg/ml, phosphate-buffer saline pH 7.3) were added to each well and the wells were incubated at 37 °C for 4 h. This colorimetric assay is based on the ability of live and metabolically unimpaired tumor-cell targets to reduce MTT to a blue formazan product. At the end of the incubation period, the supernatant was carefully aspirated, then, 100 μl of a mixture of isopropyl alcohol and 1 M hydrochloric acid (96/4, v/v) were added to each well. After 10 min of incubation and vigorous shaking to solubilize formazan crystals, the optical density was measured at 570 nm in a microculture plate reader (Dynatech MR 5000, France). For each assay, at least three experiments were performed in triplicate. The individual cell line growth curves confirmed all tumor lines in control medium remained in the log phase of cell growth 96 h after plating. Cell survival was expressed as percent of vehicle control. The IC_{50} values defined as the concentrations of drugs which produced 50% cell growth inhibition; 50% reduction of absorbance, were estimated from the sigmoidal dose-response curves.

4.2.4. *In vitro* tubulin polymerization analysis

Tubulin was prepared from pig brain according to the purification procedure described by Williams and Lee³⁵. To evaluate the effect of the compounds on tubulin assembly *in vitro*, tubulin polymerization was monitored turbidimetrically at 350 nm with a MC2 spectrophotometer (Safas, Monaco) equipped with a thermal-jacketed cuvette holder. The reaction mixture was prepared at 0 °C, and contained PEM (Pipes 0.1M, EGTA 2mM, MgSO_4 1mM pH 6.9) buffer, 25% glycerol (v/v), 1 mM GTP, MgSO_4 5mM, and 12 μM tubulin. GTP and tubulin were added at the very last minute. **EAPB0503**, its derivatives and colchicine stock solutions were diluted in DMSO to the desired concentration, and 2 μL of the compound solution was added to the medium (final concentration: 5 μM). The same volume of DMSO alone was used for negative control. The final volume of the sample was 200 μL . The reaction was started by placing the cuvette in the spectrophotometer cell compartment

thermostated at 37 °C. Ice was added 45 minutes later to initiate depolymerization to check for signal specificity.

4.2.5. Flow cytometric analysis

The cell cycle distribution was monitored by flow cytometric analysis as previously described by Brons et al³⁶. A375 cells were harvested after treatment with EABP0503, 6e or 6b for 24hh, washed with PBS and were spun down (400g, 5 min at 4°C), the supernatant was discarded, and the pellet placed on ice for 10 min. Subsequently 900 µl of an ice-cold hypotonic PI solution (221, containing 25 µg/ml Propidium iodure (Sigma), 0.1% w/v trisodium citrate dihydrate (Sigma, St louis), 10% v/v RNA-se A solution (Sigma, St. Louis) and 0.1% v/v Triton X-100 in distilled water, was added. Cells were kept overnight on ice and analyzed for DNA content. The stained cells were performed by a Gallios 10 photomultipliers (Beckman coulter) in Montpellier Rio Imaging facilities (MRI platform, Montpellier, France). The cell cycle distribution was analyzed using KALUZA flow analysis software (Beckman coulter). For each experiment, 20 000 events per sample were recorded.

4.2.6. Molecular docking analysis

The molecular modeling studies were performed with GOLD.³² The crystal structure of tubulin complexed with colchicine (PDB 4O2B)³⁷ was retrieved from the RCSB Protein Data Bank. The binding sphere with a radius of 25.0Å was defined with residue Leu255 as the binding site. All compounds were drawn with PRODRG³¹ and protonated using BABEL. Finally, they were docked into the binding site using the GOLD³² protocol with the default settings. The pictures were generated by the program PYMOL.³⁸

Acknowledgements

This work was supported by the French Infrastructure for Integrated Structural Biology (FRISBI) ANR-10-INSB-05-01. Zahraa Zghaib thanks Islamic Association for Guidance and Higher Education for its financial support. Flow cytometry was performed at MRI-Cytométrie-IRB, Institute For Regenerative Medicine and Biotherapy, Hôpital St Eloi, CHU de Montpellier.

References

1. Yaqiong, M.; Senbiao, F.; Li, L.H.; Han, C.; Lu, Y.; Zhao, Y.; Liu, Y.; Zhao, C. *Chem. Biol. Drug. Des.* 2013, 82, 12.
2. Janke, C.; Kneusse, M. *Neurosci.* 2010, 33, 362.
3. Kamal, A.; Reddy, C.R.; Vishnuvardhan, M.V.P.S.; Mahesh, R.; Nayak, V.L.; Prabhakar, S.; Reddy, C.S. *Bioorg. Med. Chem.* 2014, 24, 2309.
4. Jordan, A.; Hadfield, J.A.; Lawrence, N.J.; McGown, A.T. *Med. Res. Rev.* 1998, 18, 259.
5. Giannakakou, P.; Sackett, D.; Fojo, T. *J. Natl. Cancer Inst.* 2000, 92, 182.
6. Mishra, R.C.; Karna, P.; Gundala, S.R.; Pannu, V.; Stanton, R.A.; Gupta, K.K.; Robinson, M.H.; Lopus, M.; Wilson, L. *Biochem. Pharmacol.* 2011, 82, 110.
7. Jordan, M.A.; Wilson, L. *Nat. Rev. Cancer* 2004, 4, 253.
8. Mollinedo, F.; Gajate, C. *Apoptosis* 2003, 8, 413.
9. Zhou, J.; Giannakakou, P. *Curr. Med. Chem. Anticancer Agents* 2005, 5, 65.
10. Pasquier, E.; Honore, S.; Braguer, D. *Drug Resist. Updat.* 2006, 9, 74.
11. Zheng, C.H.; Chen, J.; Liu, J.; Zhou, X.T.; Liu, N.; Shi, D.; Huang, J.J.; Lv, J.G.; Zhu, J.; Zhou, Y.J. *Arch. Pharm. Chem. Life Sci.* 2012, 345, 454.
12. Ravelli, R.B.; Gigant, B.; Curmi, P.A.; Jourdain, I.; Lachkar, S.; Sobel, A.; Knossow, M. *Nat.* 2004, 428, 198.
13. Risinger, A.L.; Giles, F.J.; Mooberry, S.L. *Cancer Treat. Rev.* 2009, 35, 255.
14. Brossi, A.; Yeh, H.J.; Chrzanowska, M.; Wolff, J.; Hamel, E.; Lin, C.M.; Quin, F.; Suffness, M.; Silverton, J. *Med. Res. Rev.* 1988, 8, 77.
15. Bhattacharyya, B.; Panda, D.; Gupta, S.; Banerjee, M. *Med. Res. Rev.* 2008, 28, 155.
16. Paños, J.; Díaz-Oltra, S.; Sánchez-Peris, M.; García-Pla, J.; Murga, J.; Falomir, E.; Carda, M.; Redondo-Horcajo, M.; Díaz, J.F.; Barasoain, I.; Marco, J.A. *Org. Biomol. Chem.* 2013, 11, 5809.
17. Lu, Y.; Chen, J.; Xiao, M.; Li, W.; Miller, D.D. *Pharm. Res.* 2012, 29, 2943.
18. Kaur, R.; Kaur, G.; Kaur Gill, R.; Soni, R.; Bariwal, J. *Eur. J. Med. Chem.* 2014, 87, 89.
19. Lamberth, C.; Murphy Kessabi, F.; Beaudegnies, R.; Quaranta, L.; Trah, S.; Berthon, G.; Cederbaum, F.; Knauf-Beiter, G.; Grasso, V.; Bieri, S.; Corran, A.; Thacker, U. *Bioorg. Med. Chem.* 2014, 22, 3922.
20. Suman, P.; Ramalinga Murthy, T.; Rajkumar, K.; Srikanth, D.; Dayakar, C.; Kishor, C.; Addlagatta, A.; Kalivendi, S.V.; China Raju, B. *Eur. J. Med. Chem.* 2015, 90, 603.
21. Kale, S.S.; Jedhe, G.S.; Meshram, S.N.; Santra, M.K.; Hamel, E.; Sanjayan, G.J. *Bioorg. Med. Chem. Lett.* 2015, 25, 1982.
22. Beaudegnies, R.; Quaranta, L.; Murphy Kessabi, F.; Lamberth, C.; Knauf-Beiter, G.; Fraser, T. *Bioorg. Med. Chem.* 2016, 24(3), 444.
23. Kingston, D.G.I. *J. Nat. Prod.* 2009, 72, 507.
24. Becker, T.; Mahboobi, S. *Drugs Fut.* 2003, 28, 767.
25. Jordan, J.A.; Hadfield, J.A.; Lawrence, N.J.; McGown, A.T. *Med. Res. Rev.* 1998, 18, 259.
26. Moarbess, G.; Deleuze-Masquefa, C.; Bonnard, V.; Gayraud-Paniagua, S.; Vidal, J.R.; Bressolle, F.; Pinguet, F.; Bonnet, P.A. *Bioorg. Med. Chem.* 2008, 16, 6601.
27. Masquefa, C.; Moarbess, G.; Bonnet, P.A.; Pinguet, F.; Bazarbachi, A.; Bressolle, F. *U.S. Patent* 8,378,098, 2013.
28. Deleuze-Masquefa, C.; Moarbess, G.; Khier, S.; David, N.; Gayraud-Paniagua, S.; Bressolle, F.; Pinguet, F.; Bonnet, P.A. *Eur. J. Med. Chem.* 2009, 44, 3406.
29. Moarbess, G.; El-Hajj, H.; Kfoury, Y.; El-Sabban, M.E.; Lepelletier, Y.; Hermine, O.; Deleuze-Masquefa, C.; Bonnet, P.A.; Bazarbachi, A. *Blood* 2008, 111, 3770.
30. Saliba, J.; Deleuze-Masquefa, C.; Iskandarani, A.; El Eit, R.; Hmadi, R.; Mahon, F.X.; Bazarbachi, A.; Bonnet, P.A.; Nasr, R. *Anti-Cancer Drugs* 2014, 25, 624.

31. <http://www.davapc1.bioch.dundee.ac.uk/cgi-bin/prodrg>
32. PLANTS: Korb, O.; Stützel, T.; Exner, T.E. *Lect. Notes Comput. Sci.* 2006, 4150, 247.
33. La Regina, G.; Bai, R.; Coluccia, A.; Famiglini, V.; Pelliccia, S.; Passacantilli, S.; Mazzoccoli, C.; Ruggieri, V.; Verrico, A.; Miele, A.; Monti, L.; Nalli, M.; Alfonsi, R.; Di Marcotullio, L.; Gulino, A.; Ricci, B.; Soriani, A.; Santoni, A.; Caraglia, M.; Porto, S.; Da Pozzo, E.; Martini, C.; Brancale, A.; Marinelli, L.; Novellino, E.; Vultaggio, S.; Varasi, M.; Mercurio, C.; Bigogno, C.; Dondio, G.; Hamel, E.; Lavia, P.; Silvestri, R. *J. Med. Chem.* 2015, 58, 5789.
34. Hamel, E.; Lin, C.M. *Biochem.* 1984, 23 4173.
35. Williams, R.J.; Lee, J. *Methods Enzymol.*, 1982, 85B, 376.
36. Brons, P P T.; Pennings, A H M.; Haanen, C.; Wessels, H M C.; Boezeman, J B M. *Cytometry.* 1990, 11 : 837-844.
37. Prota, A.E.; Danel, F.; Bachmann, F.; Bargsten, K.; Buey, R.M.; Pohlmann, J.; Reinelt, S.; Lane, H.; Steinmetz, M.O. *J. Mol. Biol.* 2014, 426, 1848.
38. <http://pymol.sourceforge.net>

List of captions

Figure 1: Chemical structure of lead compounds.

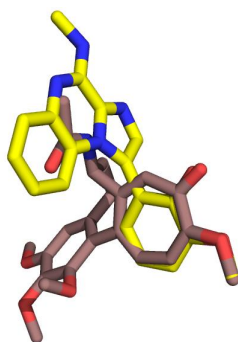
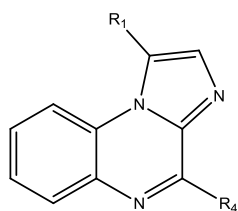
Scheme 1: Synthesis of EAPB0503 derivatives. a) EtOH, NH_2CH_3 in ethanol or NH_4OH in water, MW (180°C , 20 min); b) NBS, CHCl_3 , reflux 1h30; c) Suzuki-cross coupling ($\text{R}_1-\text{B}(\text{OH})_2$), $\text{Pd}(\text{PPh}_3)_4$, Na_2CO_3 , DME, MW (140°C , 20 min); d) Iodocyclohexane, DMF, reflux 16h.

Table 1: Imidazoquinoxalines derivatives: General formula, IC_{50} values against A375 cells and effect on tubulin polymerization inhibition.

Figure 2: EABP0503, 6b and 6e induce G2/M cell arrest on A375 cell line. (A) Effects of EABP0503, 6b and 6e on the cell-cycle distribution on A375 cell line. Treated cells were stained with PI ($25 \mu\text{g}/\text{ml}$), and the cell-analysis was performed by a Gallios flow cytometer. (B) The G0/G1, S and G2/M percentage measured in treated cells.

Figure 3: Compound 6g in the colchicine binding pocket of tubulin chains α and β . **a.** Structure of tubulin with colchicine bound PDB 4O2B; **b.** Hydrogen bonds interaction between compound 6g and tubulin (view from the top of the ligand); **c** Superposition of compound 6g and colchicine (view from the top). **d.** Superposition of compound 6g and colchicine (view from the side).; Color coding: nitrogen atoms blue, oxygen atoms red, carbon atoms pale pink for tubulin chain α , carbon atoms green for tubulin chain β , carbon atoms yellow for compound 6g and brown for colchicine; Hydrogen bonds were showed by black dash-line, the distance was denoted by Å; water molecule is shown as non-bond sphere.

Graphical abstract



6g (**R₁**: 2-OH-3-OCH₃-C₆H₃-, **R₄**: CH₃-NH-) **Superposition of 6g and colchicine**
IC₅₀ A375 = 0.077 μM
Tubulin inhibition: 90%

ACCEPTED MANUSCRIPT